

# SIMULATION OF HURRICANE RISK IN THE U.S. USING EMPIRICAL TRACK MODEL

By P. J. Vickery,<sup>1</sup> P. F. Skerlj,<sup>2</sup> and L. A. Twisdale<sup>3</sup>

**ABSTRACT:** This paper describes a new technique for modeling hurricane risk in the United States. A storm track modeling approach is employed where, for each hurricane, the entire track as it crosses the ocean and makes landfall is modeled. The central pressure is modeled as a function of the sea surface temperature. The approach is validated through comparisons of simulated and observed key hurricane statistics (central pressure, translation speed, heading, and approach distance) along the U.S. coastline. The simulated and observed landfall rates of intense hurricanes (Saffir-Simpson Scale 3 and higher) also are compared on a regional basis along the coast. The model is able to reproduce the continuously varying hurricane climatology along the U.S. coastline, and it provides a rational means for examining the hurricane risk for geographically distributed systems such as transmission lines and insurance portfolios.

## INTRODUCTION

The mathematical simulation of hurricanes is the most accepted approach for estimating wind speeds for the design of structures and assessment of hurricane risk. The simulation approach is used in the development of the design wind speed maps in the United States [American National Standards Institute (ANSI) 1982; ASCE 1990, 1996], the Caribbean [Caribbean Commodity Secretariat (CCS) 1985], and Australia [Standards Association of Australia (SAA) 1989]. The simulation approach was first described in the literature by Russell (1968, 1971) and, since that pioneering study, others have expanded and improved the modeling technique, including Batts et al. (1980), Georgiou et al. (1983), Georgiou (1985), Neumann (1991), and Vickery and Twisdale (1995b). The basic approach in all these studies is similar in that site specific statistics of key hurricane parameters including central pressure deficit, radius to maximum winds, heading, translation speed, and the coast crossing position or distance of closest approach are first obtained. Given that the statistical distributions of these key hurricane parameters are known, a Monte Carlo approach is used to sample from each distribution, and a mathematical representation of a hurricane is passed along the straight line path satisfying the sampled data while the simulated wind speeds are recorded. The intensity of the hurricane is held constant until landfall is achieved, after which the hurricane is decayed using filling rate models. As indicated in Vickery and Twisdale (1995b), the approaches used in the previously noted studies are similar, with the major differences being associated with the physical models used, including the filling rate models and wind field models. Other differences include the size of the region over which the hurricane climatology can be considered uniform (i.e., the extent of the area surrounding the site of interest for which the statistical distributions are derived) and the use of a coast segment crossing approach [e.g., Russell (1971), and Batts et al. (1980)] or a circular subregion approach [e.g., Georgiou et al.

(1983), Georgiou (1985), Neumann (1991), and Vickery and Twisdale (1995b).

In this study, a new simulation approach is developed where the full track of a hurricane or tropical storm is modeled, beginning with its initiation over the ocean and ending with its final dissipation. Using this approach, one models the central pressure as a function of sea surface temperature and updates the storm heading, translation speed, etc., at each 6-h point in the storm history. Linear interpolation is used between the 6-h points. The approach is validated by comparing the site specific statistics of the key hurricane parameters of the simulated hurricane tracks with the statistics derived from the historical data. When coupled with a hurricane wind field model [e.g., Vickery et al. (2000)], one can compute wind speeds at any point along or near the hurricane coastline. Finally, in this study, the intensity of each simulated hurricane that makes landfall is computed and the statistics of the intense hurricanes (IHs) (Saffir-Simpson Scale 3 and higher) are compared with the historical statistics.

## EMPIRICAL STORM MODELING APPROACH

### Storm Track Modeling

Using the storm track modeling technique, the number of storms to be simulated in any year is obtained by sampling from a negative binomial distribution having a mean value of 8.4 storms/year and a standard deviation of 3.56 storms/year. The starting position, date, time, heading, and translation speed of all tropical storms as given in the HURDAT database (Jarvinen et al. 1984) are sampled from and used to initiate the simulation. Using the historical starting position, date, and time of the storms ensures that the climatology associated with any seasonal preferences for the point of storm initiation is retained. Given the initial storm heading, speed, and intensity, the simulation model estimates the new position and speed of the storm based on the changes in the translation speed and storm heading over the current 6-h period. The changes in the translation speed  $c$  and storm heading  $\theta$  between times  $i$  and  $i + 1$  are obtained from

$$\Delta \ln c = a_1 + a_2\psi + a_3\lambda + a_4 \ln c_i + a_5\theta_i + \varepsilon \quad (1a)$$

$$\Delta \theta = b_1 + b_2\psi + b_3\lambda + b_4c_i + b_5\theta_i + b_6\theta_{i-1} + \varepsilon \quad (1b)$$

where  $a_1, a_2$ , etc. = constants;  $\psi$  and  $\lambda$  = storm latitude and longitude, respectively;  $c_i$  = storm translation speed at time step  $i$ ;  $\theta_i$  = storm heading at time step  $i$ ;  $\theta_{i-1}$  = heading of the storm at time step  $i - 1$ ; and  $\varepsilon$  = random error term. The coefficients  $a_1, a_2$ , etc., have been developed using  $5^\circ \times 5^\circ$  grids over the entire Atlantic Basin. A different set of coefficients for easterly and westerly headed storms is used. As the

<sup>1</sup>Sr. Engr., Applied Research Associates, 811 Spring Forest Rd., Ste. 100, Raleigh, NC 27609.

<sup>2</sup>Staff Engr., Applied Research Associates, 811 Spring Forest Rd., Ste. 100, Raleigh, NC.

<sup>3</sup>Prin. Engr., Applied Research Associates, 811 Spring Forest Rd., Ste. 100, Raleigh NC.

Note. Associate Editor: Timothy A. Reinhold. Discussion open until March 1, 2001. Separate discussions should be submitted for the individual papers in this symposium. To extend the closing date one month, a written request must be filed with the ASCE Manager of Journals. The manuscript for this paper was submitted for review and possible publication on January 26, 1998. This paper is part of the *Journal of Structural Engineering*, Vol. 126, No. 10, October, 2000. ©ASCE, ISSN 0733-9445/00/0010-1222-1237/\$8.00 + \$.50 per page. Paper No. 17443.

simulated storm moves into a different  $5^\circ \times 5^\circ$  square, the coefficients used to define the changes in heading and speed change accordingly. In the case of grid squares with little or no historical data (e.g., East Atlantic Ocean and squares near the equator), the coefficients in (1) for these squares are assigned the values for those determined for the nearest grid square.

### Central Pressure Modeling

The central pressure of a storm is modeled here through the use of a relative intensity parameter that is coupled to the sea surface temperature. Modeling hurricanes using this relative intensity concept was first used in single-point simulations by Darling (1991). Note that, although the actual central pressure of a hurricane is a function of more than the sea surface temperature (e.g., wind shear aloft, storm age, and depth of warm water), the modeling approach is an improvement over traditional simulation techniques in that the derived central pressures are bounded by physical constraints, thus eliminating the need to artificially truncate the central pressure distribution. The introduction of sea surface temperature into the modeling process also reduces some of the unexplained variance in the central pressure modeling that would exist if the model was developed using central pressure data alone. Fig. 1 shows example plots of central pressure deficit  $\Delta p$  and the relative intensity parameter  $I$  versus sea surface temperature for hurricanes in the Gulf of Mexico (in Fig. 1, hurricanes are defined as having a  $\Delta p$  of 25 mbar or greater). As indicated in Fig. 1, the correlation between  $\Delta p$  and sea surface temperature increases with increasing  $\Delta p$ , whereas the correlation between  $I$  and sea surface temperature is weak.

The relative intensity approach is based on the efficiency of a tropical cyclone relative to a Carnot cycle heat engine, and

the details of the approach given in Darling (1991) are not repeated here. To compute  $I$  of a hurricane, one uses the mean monthly sea surface temperatures in the Atlantic Basin (given in  $1^\circ$  squares) at the location of the storm, combined with the central pressure data given in the HURDAT database [see description in Jarvinen et al. (1984)], an assumed relative humidity of 0.75, and a temperature at the top of the stratosphere taken to be equal to 203°K (Emanuel 1988). Using the approach given in Darling (1991), every central pressure measurement given in HURDAT is converted to a relative intensity.

During the hurricane simulation process, the values of  $I$  at each time step are obtained from

$$\ln(I_{i+1}) = c_0 + c_1 \ln(I_i) + c_2 \ln(I_{i-1}) + c_3 \ln(I_{i-2}) + c_4 T_s + c_5 (T_{s_{i+1}} - T_{s_i}) + \varepsilon \quad (2)$$

The coefficients  $c_0$ ,  $c_1$ , etc., vary with storm latitude, storm intensity, basin (Gulf of Mexico or Atlantic Ocean), and heading (i.e., easterly or westerly direction). Near the U.S. coastline, where more continuous pressure data is available, finer, regionally specific values of these coefficients are developed. These regionally specific coefficients take into account changes in the relationships between sea surface temperature and storm intensity that are influenced by subsurface water temperatures, as described for example in Chouinard et al. (1997). These regional coefficients preserve the variations in local hurricane climatology along the coastline. In the modeling process, once a simulated storm makes landfall, the reduction in central pressure with time is modeled using the filling models described in Vickery and Twisdale (1995a). If a storm moves back over water, (2) is again used to model the variation in central pressure with time.

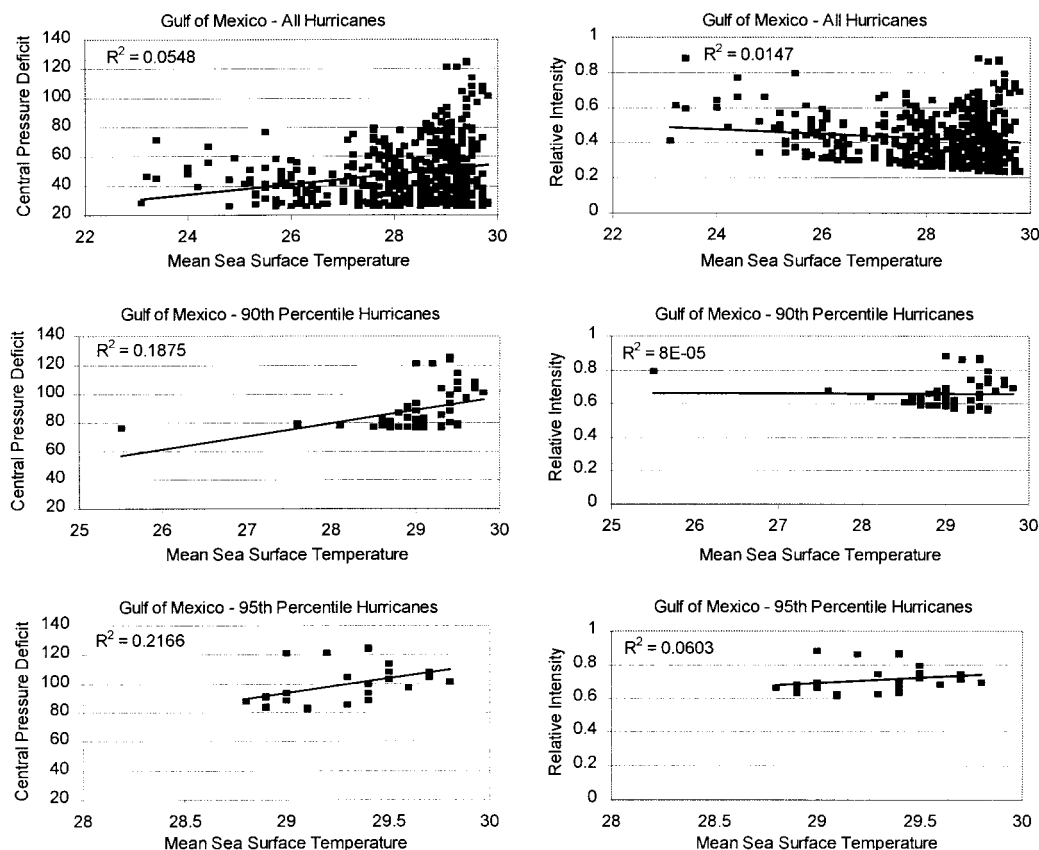


FIG. 1. Examples of Central Pressure Deficit (millibar) and Relative Intensity versus Sea Surface Temperature for Hurricanes in Gulf of Mexico

## EVALUATION OF STORM TRACK AND CENTRAL PRESSURE MODEL

The hurricane modeling methodology described above is evaluated through comparisons of observed and simulated hurricane statistics along the Mexico-U.S. coastline. The simulated statistics are derived from a 20,000-year simulation of storms occurring in the Atlantic Basin. The storms are initializing over water using the HURDAT data as indicated earlier and propagated over the ocean using (1) and (2) to define their position and intensity. Comparisons are given for the statistics of simulated and real storms that approach within 250 km of the coastal mileposts (MPs) shown in Fig. 2. The central pressure difference statistics are computed using the minimum values observed within the 250-km-radius subregion. All other parameters are those computed or observed at the point of closest approach to the MP.

Fig. 3 shows comparisons of the mean and, in some cases, standard deviation of the simulated and observed values of heading, translation speed, minimum approach distance, occurrence rate, and central pressure along the Mexican and U.S. coastlines. The minimum approach distance  $d_{\min}$  is defined as positive if a storm passes to the right of a site and negative if

the storm passes to the left. The HURDAT statistics given in Fig. 3 are derived for storms occurring during the period 1886–1996. In Fig. 3, if the mean value of  $d_{\min}$  is negative, the storms pass to the left of a given MP on average. The comparison of simulated and observed hurricane statistics shown in Fig. 3 indicates that the modeling approach provides good estimates of the five key hurricane parameters at most locations along the coastline. Standard statistical tests (i.e.,  $t$ -test and  $F$ -test) are performed to test for the equivalence of the simulated and observed estimates of the mean and standard deviations of the key hurricane parameters on an MP-by-MP basis. A total of 74 MPs are used along the coastline with 100-nautical-mile ( $\sim 185$ -km) spacing used along the Mexican coastline and 50-nautical-mile ( $\sim 93$ -km) spacing used on the U.S. coastline. Table 1 presents the MP locations where the  $t$ -tests performed to determine the equivalence of means fail. Table 2 presents the MP locations where the  $F$ -tests performed to determine the equivalence of variances fail.

The large number of failed variance equivalence tests for the translation speed and storm heading was of concern and prompted further study. Fig. 4 shows a comparison of the log-normal distributions used to fit the simulated translation speed data along with the frequency histograms of the observed

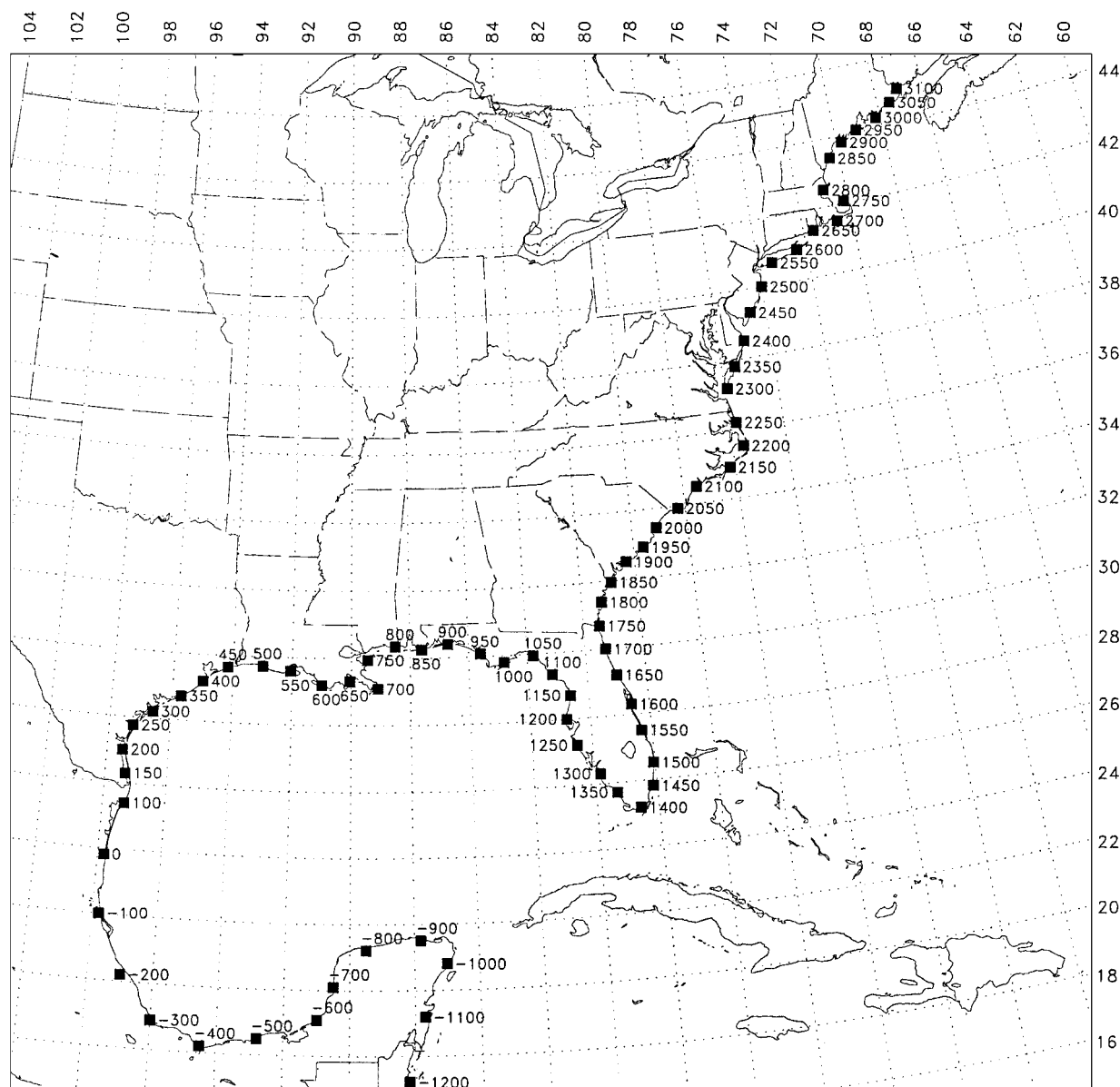


FIG. 2. Locations of MPs along U.S. and Mexican Coastline Used in Study

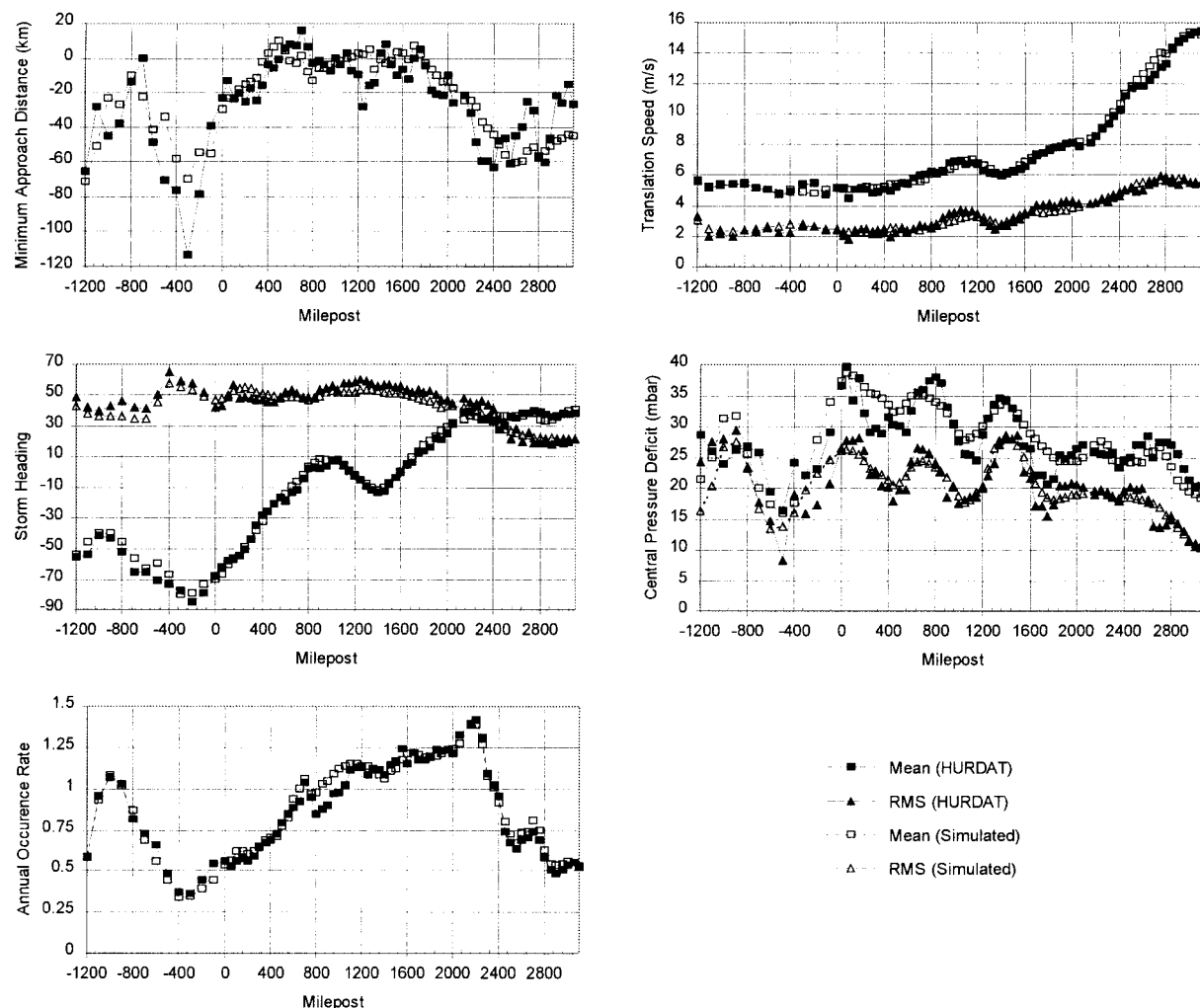


FIG. 3. Comparison of Simulated and Observed Key Hurricane Parameters at 100-Nautical-Mile Increments along U.S. and Mexican Coastline

TABLE 1. Number of Locations Where *t*-Tests Performed for Determining Equivalence of Means Failed

Parameter (1)	5% Confidence Level		1% Confidence Level	
	N (2)	MPs (3)	N (4)	MPs (5)
Minimum approach distance	3	-500, -300, 1,250	0	N/A
Translation speed	1	100	0	N/A
Storm heading	1	2,450	0	N/A
Central pressure deficit	2	1,650, 1,750	0	N/A
Occurrence rate	0	N/A	0	N/A

Note: N/A = not applicable.

translation speed data for the seven locations where the *F*-tests failed along the U.S. coastline. The fit to the simulated data passed the chi-squared goodness-of-fit test at the 5% confidence level (comparing with the observed data) in all cases examined.

In the case of the storm heading, the grouping of the failed variance equivalence tests in the 2,150–2,250-nautical-mile (3,982–4,723 km) range was a concern and was examined further using a similar approach to that used in the case of the translation speeds. Fig. 5 shows a comparison of the distributions of the observed and simulated headings (or approach angles) at MPs 2,150, 2,300, 2,350, and 2,400.

The analytic distributions are fit to the simulated data and shown plotted against both the simulated and the observed

TABLE 2. Number of Locations Where *F*-Tests Performed for Determining Equivalence of Variances Failed

Parameter (1)	5% Confidence Level		1% Confidence Level	
	N (2)	MPs (3)	N (4)	MPs (5)
Minimum approach distance	2	-1,200, -500	0	N/A
Translation speed	9	-1,100, -900, 100, 450, 900, 950, 1,000, 1,350, 1,800	2	-1,100, 100
Storm heading	10	-900, -800, -700, 1,850, 2,150, 2,300, 2,350, 2,400, 2,550, 2,650	4	-800, 2,300, 2,350, 2,400
Central pressure deficit	2	-1,100, -500	0	N/A

Note: N/A = not applicable.

data. As can be seen, the distributions derived from the simulated data describe the observed data remarkably well. The differences in the variances evident in the *F*-tests are associated with a relatively small number of storms that approach the coast in this region traveling in a south-southeasterly direction. These storms exist in the simulation but occur less frequently than those observed in nature.

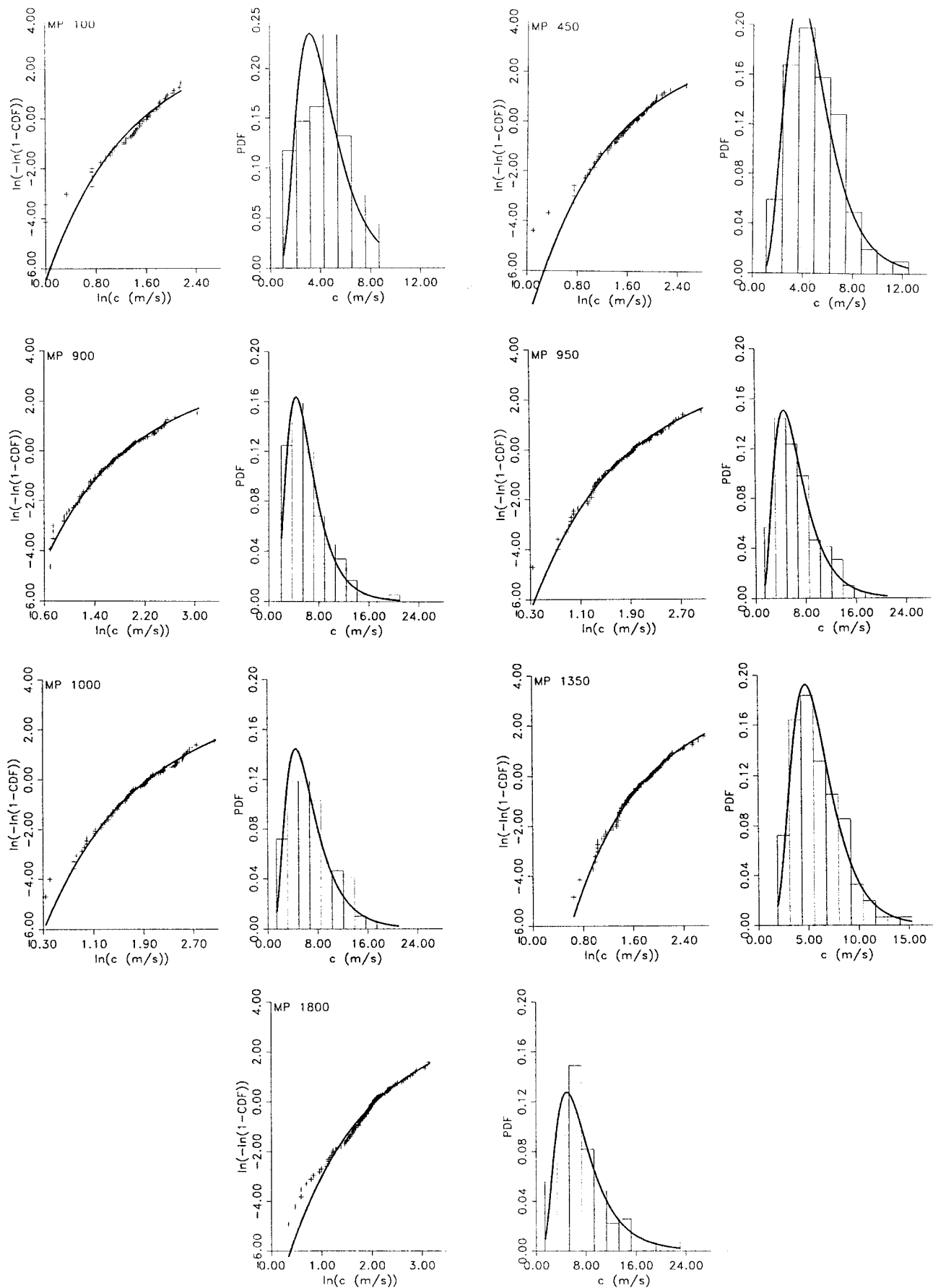
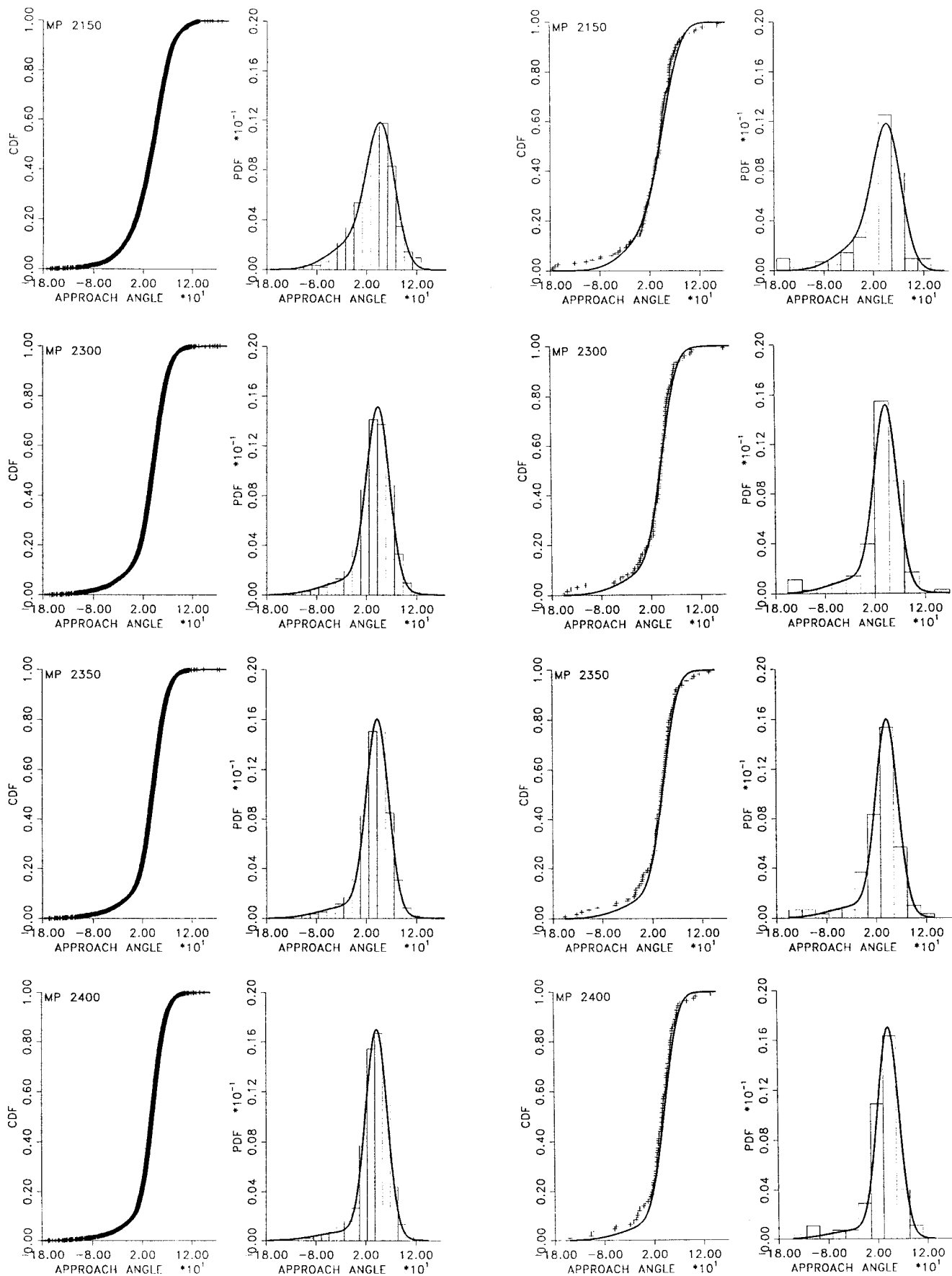
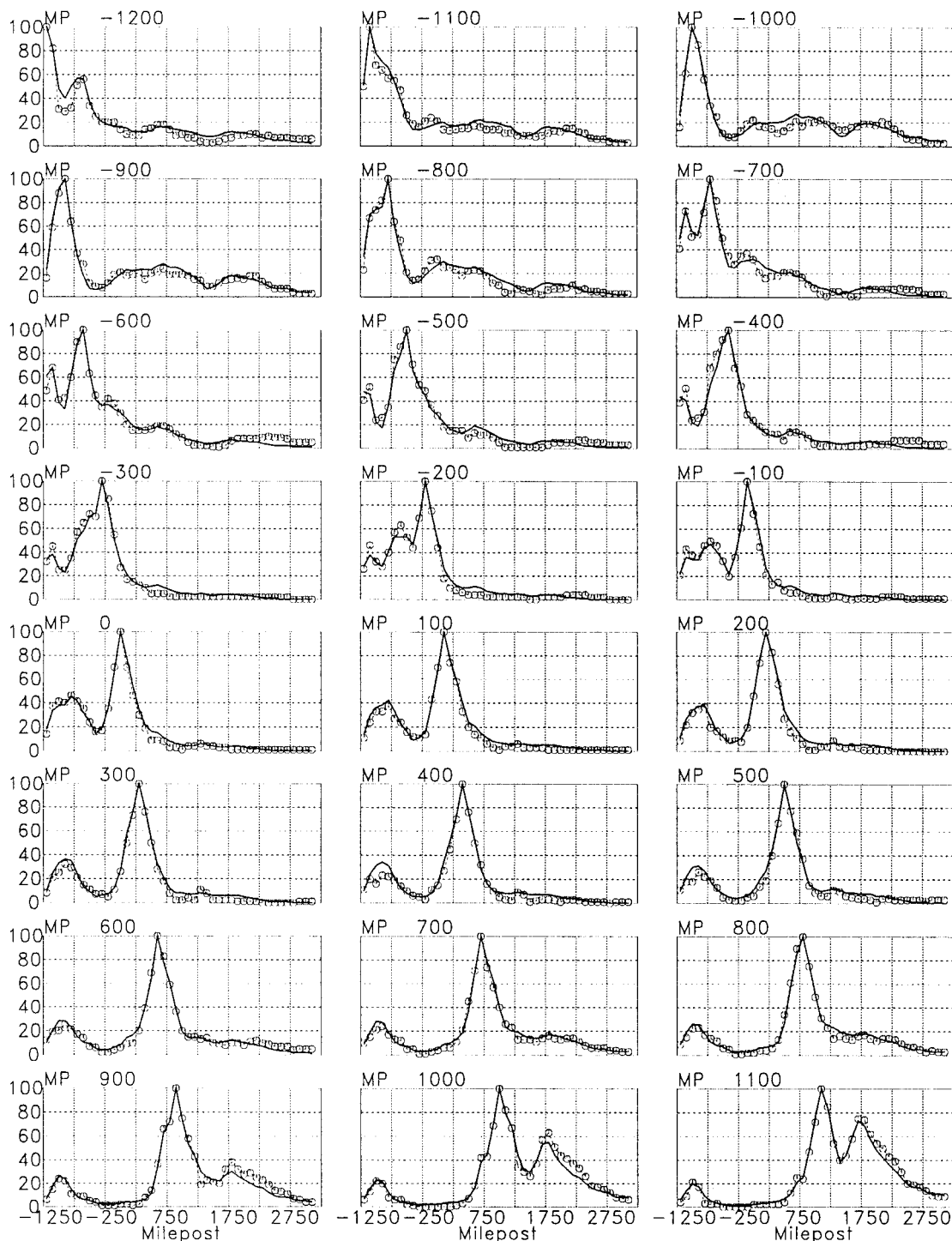


FIG. 4. Comparison of Simulated and Observed Distributions for Translation Speed  $c$  at Selected MPs along U.S. Coastline (Distribution Fit to Simulated Data Shown as Solid Line, Points and Bars are Observed Data) (CDF = Cumulative Distribution Function; PDF = Probability-Density Function)



**FIG. 5. Comparison of Simulated and Observed Distributions for Storm Heading (Approach Angle) at MPs along Mid-Coastline [Solid Line (in All Cases) Represents Distribution Fit to Simulated Data, Points and Bars Presented in Plots on Left Side Are from Simulated Data, Points and Bars Presented in Plots on Right Side Are from Observed Data (i.e., HURDAT)] (CDF = Cumulative Distribution Function; PDF = Probability-Density Function)**



**FIG. 6. Conditional Probabilities Comparing Probability of Tropical Storms Passing within 250 km of MP  $i$  and MP  $j$  Derived from Simulations and Observations (Simulated Data Shown as Solid Line)**

Fig. 6 presents, on an MP-by-MP basis [spaced at 100 nm (185.2 km)], a comparison of the simulated and observed fraction of storms that pass within 250 km of MP  $i$  and also pass within 250 km of MP  $j$ . For example, as indicated in Fig. 6, at MP 1,300, approximately 50% of the simulated storms that pass within 250 km of this MP also pass within 250 km of MP 1,700. These comparison data were tested for their statistical equivalence of proportions. The test was applied to the 1,308 cases shown in Fig. 6 for which the fraction falls in the range [0.05, 0.95]. At the 5% confidence level, one expects that for 1,308 tests drawn randomly from a population of such tests, on average 65 (i.e., 5%) would fail. Using a 1% confidence level, the expected number of failed tests is 13. With

the set of 1,308 tests, 47 fail at the 5% confidence level and 12 fail at the 1% confidence level. From this it has been concluded that the modeled probability of a hurricane entering a 250-km-radius subregion centered on MP  $i$  and also passing through the same size subregion centered on MP  $j$  is adequately modeled using this simulation methodology. In other words, the tracks of the storms are well modeled near the coastline.

An advantage of the storm track modeling approach over the circular subregion approach results from not having to rely on an assumption of uniform climatology over the subregion. This assumption can cause anomalous simulations in the subregion approach. For example, for MPs located on the East

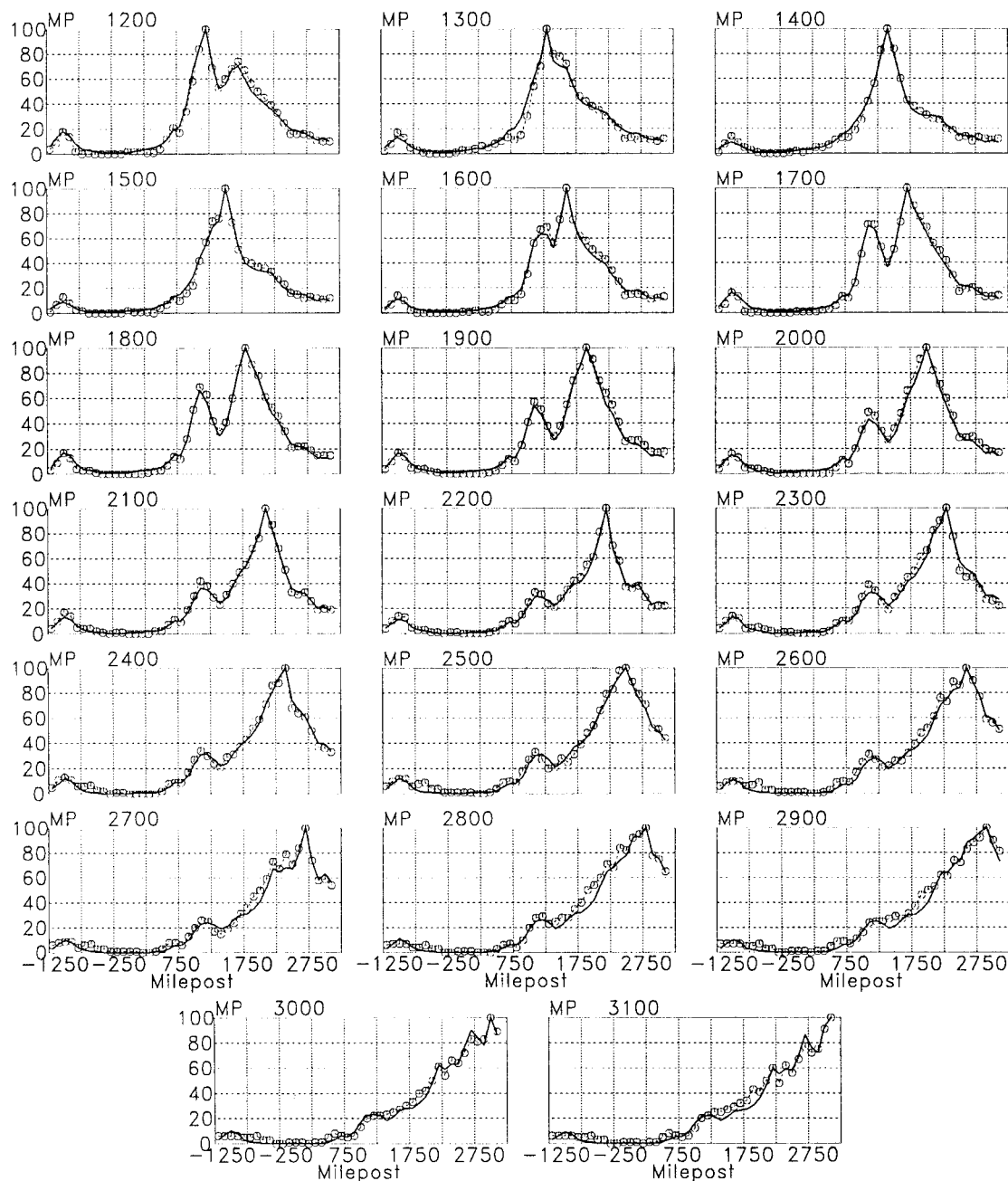


FIG. 6. (Continued)

Coast of the United States and much of the Gulf Coast, when sampling from the distributions for  $d_{\min}$ ,  $\Delta p$ , and  $\theta$ , it is possible to sample intense storms that are initiated on land. In an attempt to eliminate this problem, Vickery and Twisdale (1995b) modeled  $\Delta p$  as a function of  $\theta$  for East Coast locations. The storm modeling approach described here eliminates this sampling problem, because any storm that enters a sub-region from land will have been weakened by the filling models. The uniformity assumption associated with the sub-region approach is likely to be even more significant in the case of inland sites, where the climatology will vary significantly within the subregion.

The empirical storm track modeling approach has been shown to successfully reproduce the statistics of the key hurricane parameters along the U.S. coastline, and the approach is able to properly model the probabilities of a single storm passing near multiple sites. Using this simulation procedure, the storm intensities change with time and the storms change both direction and speed as they pass by a site. This more

realistically models storm paths when compared to traditional hurricane simulation methods.

## MODELING OF RADIUS TO MAXIMUM WINDS AND HOLLAND'S PRESSURE PROFILE PARAMETER (HOLLAND 1980)

### Radius to Maximum Winds

The two models of the radius to maximum winds given in Vickery and Twisdale (1995b) have been revisited to develop a single model for use along the entire coastline of the United States. Radius to maximum winds  $R_{\max}$ , latitude  $\psi$ , and central pressure deficit  $\Delta p$  data obtained from eight additional storms were added to the data used in Vickery and Twisdale (1995b), which were obtained from Ho et al. (1987). The models for  $R_{\max}$  given in Vickery and Twisdale (1995b) are

$$\ln R_{\max} = 3.853 - 0.0061\Delta p, \quad r^2 = 0.0701 \quad (3)$$



**TABLE 3. Comparison of  $R_{\max}$  Models for Storms South of 30° N**

Equation (1)	$r^2$ (2)	$\epsilon$ [ln(km)] (3)
5	0.0973	0.4225
7	0.1421	0.4164
8	0.1899	0.4046
9	0.1044	0.4494

**TABLE 4. Comparison of  $R_{\max}$  Models for Storms North of 30° N**

Equation (1)	$r^2$ (2)	$\epsilon$ [ln(km)] (3)
6	0.0859	0.3690
7	0.0791	0.3778
8	0.0319	0.3870
9	0.0814	0.3394

for storms located south of 30° N and

$$\ln R_{\max} = 2.395 + 0.0426\psi, \quad r^2 = 0.1460 \quad (4)$$

for storms located north of 30° N.

Using the same approach, but with the updated database, these models become

$$\ln R_{\max} = 3.919 - 0.00737\Delta p, \quad r^2 = 0.0973 \quad (5)$$

for storms south of 30° N and

$$\ln R_{\max} = 2.569 + 0.037842\psi, \quad r^2 = 0.0859 \quad (6)$$

for storms located north of 30° N.

For use in the storm track modeling approach, three new candidate global models for  $R_{\max}$  were developed. These are

$$\ln R_{\max} = 2.636 - 0.00005086\Delta p^2 + 0.0394899\psi, \quad r^2 = 0.2765 \quad (7)$$

$$\ln R_{\max} = 2.097 + 0.0187793\Delta p - 0.00018672\Delta p^2 + 0.0381328\psi, \quad r^2 = 0.2994 \quad (8)$$

$$\ln R_{\max} = 2.713 - 0.0056748\Delta p + 0.0416289\psi, \quad r^2 = 0.2544 \quad (9)$$

Based on the  $r^2$  values, the models given in (7)–(9) are superior to any of the models given in (3) and (4) or (5) and (6).

To compare the new  $R_{\max}$  models on the same regional basis used to develop the Vickery and Twisdale (1995b) models, the new models were used to examine the reduction in variance for the two regions examined separately. Results of the comparisons are given in Tables 3 and 4.

In Tables 3 and 4,  $\epsilon$  represents the standard deviation of the difference between the predicted and observed values of  $\ln(R_{\max})$ . Comparing the  $r^2$  values given in Tables 3 and 4, it is clear that, although the overall reduction in the unexplained variance obtained using (8) is greater than that obtained using either (7) or (9), this model does not perform well for storms located north of 30° N. The  $R_{\max}$  model described in (7) was found to be the best compromise for a single model to be used for simulations in the Atlantic Basin.

### Holland's Radial Pressure Profile Parameter

Upper-level aircraft data provided by H. Willoughby of the Hurricane Research Division (HRD) of the National Oceanic and Atmospheric Administration (NOAA) were used to determine representative values of the Holland radial pressure pro-

file parameter (Holland 1980)  $B$  for a total of 1,300 radial profiles in 27 hurricanes. Radial profile data were measured at constant pressure levels of 500, 600, 700, 850, and 900 mbar. Two methods are employed to estimate the Holland parameter for a given profile. The first uses the aircraft pressure data and the second uses the aircraft upper-level wind speed data.

### Estimates of Holland's Profile Parameter from Surface Pressure Data

Organized according to their radial distance from the storm center, aircraft data including flight pressure, flight altitude, dew-point temperature, and air temperature are used to estimate the surface pressure. The surface pressure is computed hydrostatically using thermodynamic quantities appropriate for the intervening layer between the surface and flight level. The radial distribution of surface pressure for a given case is then compared to the following expression:

$$p(r) = p_0 + \Delta p \exp \left[ - \left( \frac{A}{r} \right)^B \right] \quad (10)$$

where  $p(r)$  = surface pressure at a distance  $r$  from the storm center;  $p_0$  = central pressure;  $A$  = location parameter; and  $B$  is Holland's pressure profile parameter. Rearranging the above expression and taking the double natural logarithm leads to

$$\ln \left[ -\ln \left( \frac{p(r) - p_0}{\Delta p} \right) \right] = -B \ln(r) + B \ln(A) \quad (11)$$

The surface pressure and radial distance data are transformed to the above form, and a regression analysis is used to obtain estimates of  $B$ .

Results show that a large portion of the surface pressure distributions cannot be adequately modeled with the pressure profile described with a single value of  $B$ . Considering only those profiles where the flight pressure is 700 mb or higher (i.e., heights of approximately 3,000 m or less) and  $\Delta p > 25$  mb, it was found that about 60% of the fits yield  $r^2$  values  $> 0.98$ . Storm profiles for which the model is inadequate include those exhibiting double eye walls (e.g., Alicia and Allen) and those that are very intense and tight (e.g., Gilbert and Allen). In general, the ability of (10) to describe the variation in the pressure field over the full domain of the storm is limited, and this is discussed further in Thompson and Cardone (1996). In the case of the very intense and tight storms such as Gilbert in 1988 and Allen in 1980, estimating  $B$  from the pressure profile yields an underestimate of the true value of  $B$ , which drives the maximum winds within the storm. This underestimate is brought about by the fact that  $B$  varies significantly between the center of the storm to a distance of about  $2R_{\max}$  from the center. Over this range, it was not uncommon to see three distinct slopes of the double logarithmic transform as described by (11). To overcome this problem, the pressure and wind profiles were reexamined to extract an effective value of  $B$  using the upper-level wind speed data.

### Estimates of Holland's Profile Parameter from Upper-Level Wind Speed Data

An alternate approach for estimating an effective value of  $B$  is to compare the upper-level wind speed data with the wind speeds derived from the gradient balance equation

$$\frac{1}{\rho} \frac{\partial p(r)}{\partial r} = \frac{V^2}{r} + fV \quad (12)$$

where  $V$  = gradient wind speed;  $f$  = Coriolis parameter; and  $\rho$  = air density. To account for the asymmetry in wind speeds resulting from the storm translation speed, Blaton's adjusted radius of curvature is used (Georgiou 1985)

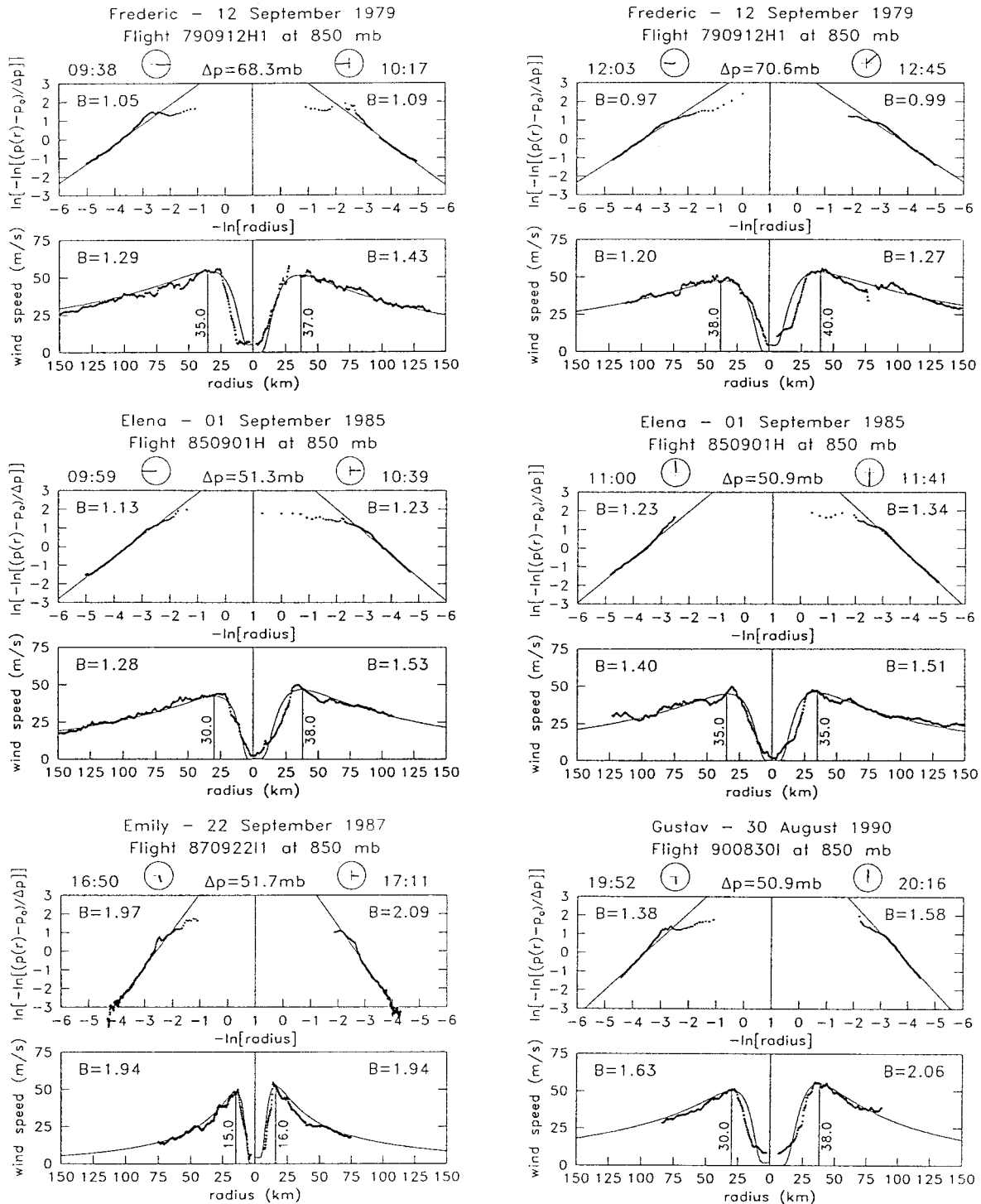


FIG. 7. Comparisons of Holland's  $B$  Parameters Derived from Pressure and Velocity Fields

$$r_i = \frac{r}{1 - \frac{c}{V} \sin(\alpha)} \quad (13)$$

where  $\alpha$  = angle (positive clockwise) from the storm translation direction to the profile location. Substituting (10) into (12) and replacing  $r$  with  $r_i$  leads to the following expression for gradient wind speeds:

$$V = \frac{1}{2} (c \sin(\alpha) - fr) + \sqrt{\frac{1}{4} (c \sin(\alpha) - fr)^2 + \frac{B\Delta p}{\rho} \left(\frac{A}{r}\right)^B \exp\left[-\left(\frac{A}{r}\right)^B\right]} \quad (14)$$

For each radial profile, mean values of  $c$ ,  $\alpha$ , and  $f$  are determined together with the flight-level values of  $\rho$  and  $\Delta p$ . The location parameter  $A$  is taken as the radius to maximum winds, which is visually assessed on a profile-by-profile basis from the flight-level wind speed data. Values of  $B$  are chosen so that the model well describes the measured wind speeds in the vicinity of  $R_{\max}$ . The algorithm obtains the most appropriate  $B$  value by minimizing the sum of the square differences between the measured and modeled wind speeds for ranges no larger than  $0.5R_{\max} - 2R_{\max}$ . Also, the square differences closer to  $R_{\max}$  were given more weight. This approach yields radial wind speed profiles that reproduce the observed profiles much better than those derived using the measured pressures directly. Fig. 7 shows examples of cases where using the Holland pres-

sure model to describe the variation of central pressure is poor, but the effective values of  $B$  computed using the approach described above yield good representations of the upper-level hurricane wind field.

Using the estimates of the effective values of  $B$  derived for storms with  $\Delta p > 25$  mb and flight levels  $< 3,000$  m, one finds that  $B$  varies with  $\psi$ ,  $\Delta p$ , and  $R_{\max}$ . The resulting model for  $B$  is

$$B = 1.34 + 0.00328\Delta p - 0.00522R_{\max}, \quad r^2 = 0.076 \quad (15)$$

Using the estimates of the effective value of  $B$  derived for storms with  $\Delta p > 25$  mb and flight levels  $< 1,500$  m, one again finds that  $B$  varies with  $\psi$ ,  $\Delta p$ , and  $R_{\max}$ . The resulting model for  $B$  is

$$B = 1.38 + 0.00184\Delta p - 0.00309R_{\max}, \quad r^2 = 0.026 \quad (16)$$

Note that in (15) and (16), the dependence of  $B$  on latitude  $\psi$  is included through the dependence of  $R_{\max}$  on latitude as defined in (7). Eq. (16) was selected to model  $B$  primarily because the pressures and wind speeds measured at the lower levels (i.e., 1,500 m versus 3,000 m) are more representative of the pressure field and gradient velocity field that drive the surface-level wind speeds. Although the correlation between  $B$  and both  $\Delta p$  and  $R_{\max}$  is relatively weak, the decision to maintain the correlation was based primarily on the upper-level data obtained for Hurricanes Gloria in 1985 and Bob in 1991. These two examples provided the only information on  $B$  for storms in northern latitudes, where  $B$  decreased notably as the storms moved north, decreased in intensity, and increased in size.

## COMPARISONS OF SIMULATED AND OBSERVED FREQUENCY OF INTENSE LANDFALLING HURRICANES

The historical information on the frequency of landfalling IHs along the coastline provides another means to evaluate the hurricane simulation model. The IHs are defined as hurricanes rated as a category 3–5 on the Saffir-Simpson Scale (Table 5). During the simulation process, when any simulated storm makes landfall (defined here as when a simulated storm track crosses the modeled coastline, which includes the Florida Keys and the outer banks of North Carolina), the central pressure, maximum sustained wind speed (1-min average, over water), and landfall location are retained. Using the magnitude of the central pressure and peak sustained wind speed at the time of landfall, the simulated storm is assigned a Saffir-Simpson category as defined by Table 5. The magnitude of the wind speed is computed using the wind field model described in Vickery et al. (2000). Figs. 8 and 9 show comparisons of the simulated and observed landfall rates by region of IHs. The simulated landfall rates were determined from a 20,000-year simulation. Fig. 8 presents simulated storms categorized by central pressure, whereas Fig. 9 presents simulated storms categorized by wind speed. The observed data are presented as the mean value  $\pm 1.96\sigma_{\mu}$ , where  $\sigma_{\mu}$  is the standard error in the mean (i.e., the range represents the 95% confidence interval). In the case of storms that made multiple landfalls, the data given in Hebert et al. (1997) was reviewed along with the estimated wind speeds and central pressures given in the HURDAT database to confirm the category of the storm at both landfall locations. For example, Hurricane Andrew is scored as a single category

TABLE 5. Saffir-Simpson Storm Categories

Saffir-Simpson category (1)	Minimum central pressure (mbar) (2)	Maximum sustained wind speed (over water) [m/s (mph)] (3)	Maximum gust speed (over water) [m/s (mph)] (4)	Maximum gust speed (over land, $z_0 = 0.03$ m) [m/s (mph)] (5)
1	$\geq 980$	33.1–42.0 (74–94)	40.6–51.9 (91–116)	36.8–48.1 (82–108)
2	979–965	42.0–49.6 (94–110)	51.9–61.7 (116–140)	48.1–58.1 (108–130)
3	964–945	49.6–58.1 (110–130)	61.7–72.7 (140–165)	58.1–69.7 (130–156)
4	944–920	58.1–69.3 (130–155)	72.7–87.3 (165–195)	69.7–85.5 (156–191)
5	$< 920$	$> 69.3$ ( $> 155$ )	$> 87.3$ ( $> 195$ )	$> 85.5$ ( $> 191$ )

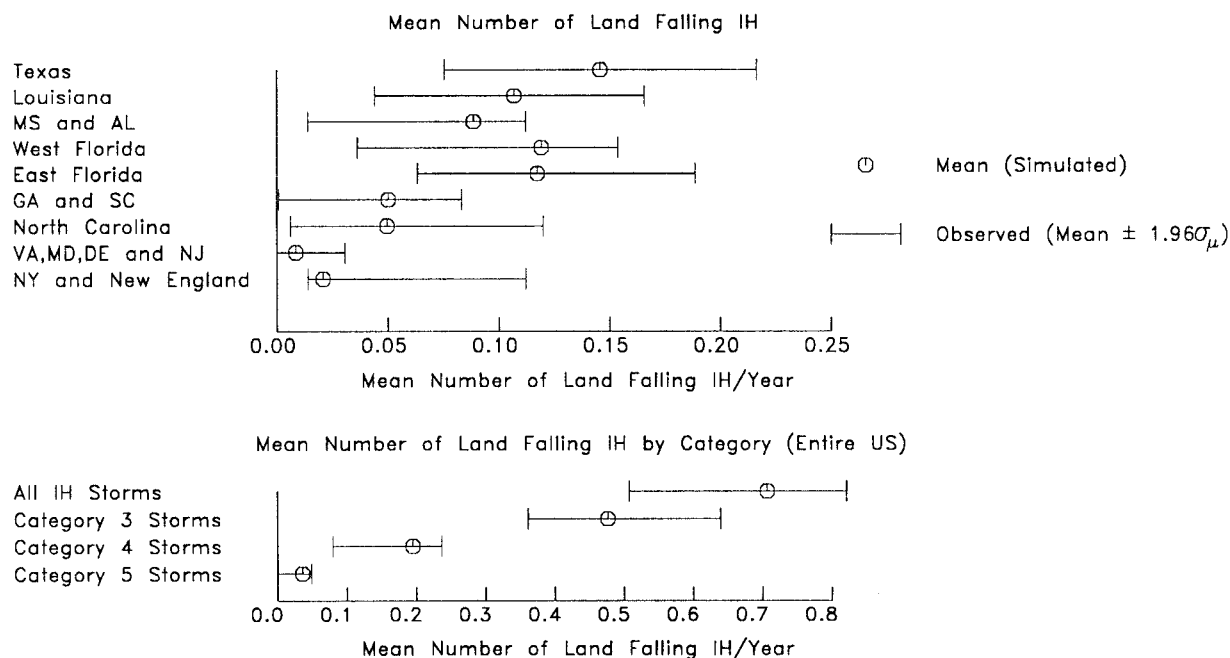
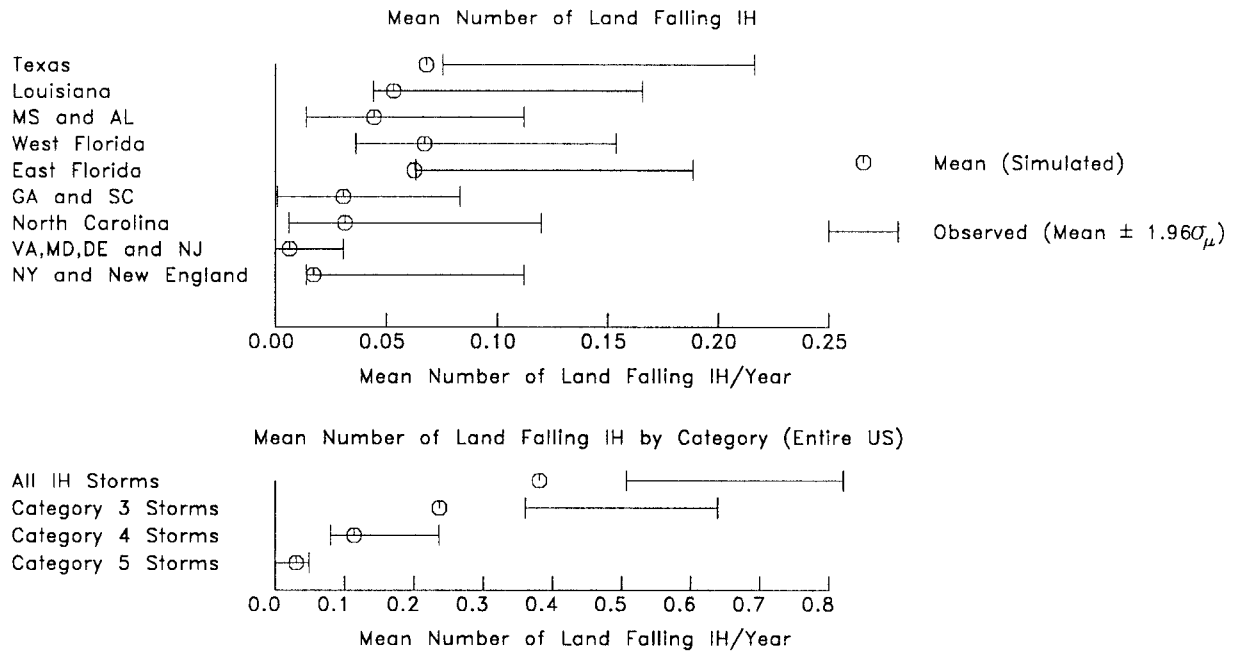


FIG. 8. Comparison of Number of Annual Landfalling IHs (Simulated Hurricane Intensity Defined by Central Pressure)



**FIG. 9. Comparison of Number of Annual Landfalling IHs (Simulated Hurricane Intensity Defined by Maximum Sustained Wind Speed)**

4 storm; however, the storm made landfall in South Florida as a category 4 storm and then proceeded to make landfall as a category 3 storm in Louisiana. A number of other storms also made landfall at more than one location. Some storms, such as Hurricane Emily in 1993, which did not actually make landfall as defined in the simulation procedure but are included in Hebert et al. (1997), were removed. Hurricane Diana in 1984 is scored in Hebert et al. (1997) as a category 3 storm, but this storm, which finally made landfall as a category 2 storm, also was removed from the data set.

As indicated in Fig. 8, the simulated hurricanes categorized by central pressure agree well with historical observation. The category definitions of the landfalling hurricanes as given in Hebert et al. (1997) are consistent with the category of the storm that would be assigned given the central pressure of the storm at the time of landfall. This consistency is important because the magnitude of the minimum central pressure is usually known with a high degree of confidence (unlike the magnitude of the maximum wind speed) at the time of landfall. Given that the definition of the hurricane category as defined by its central pressure at the time of landfall is reliable, the agreement between the simulated storms categorized by central pressure and observed frequency of IHs along the U.S. coastline, as shown in Fig. 8, lends further confidence to the hurricane simulation technique described herein.

The comparisons of historical and observed IHs where the categories of the simulated storms are determined by the simulated sustained (1-min average) wind speed (Fig. 9) suggest that the model results underestimate the occurrence of IHs striking the United States. Table 6 shows a comparison of the Saffir-Simpson rating of recent landfalling storms that have been followed by detailed studies of the wind field at the time of landfall. All of the reconstructed wind fields were produced by NOAA/HRD, the results of which are given in Powell (1987), Powell et al. (1991), Powell and Houston (1996, 1998), and Houston et al. (1997). As indicated in Table 6, the official rating (defined by wind speed) given to many of the hurricanes is high, with most of these overratings occurring when category 2 storms are scored as category 3 storms. At least 50% of the category 3 storms given in Table 6 are overrated by one category. In the case of the Hurricane Alicia surface wind field analysis given in Powell (1987), the averaging

**TABLE 6. Comparison of NHC Hurricane Classifications to Classifications Resulting from Detailed Studies Performed by NOAA/HRD**

Hurricane (1)	Year (2)	NHC category at landfall (3)	Category by central pressure at landfall (4)	Category by maximum wind speeds at landfall (NOAA/HRD) (5)
Frederic	1979	3	3	3
Alicia	1983	3	3	1–2
Hugo	1989	4	4	4
Andrew	1991	4	4	4
Emily	1993	3	3	3
Erin	1995	1	1	1
Opal	1995	3	3	2
Bertha	1996	2	2	2
Fran	1996	3	3	2

time is not explicitly stated, although a 1-min average is implied. The maximum surface-level wind speed given in Powell (1987) for Alicia at landfall is 39 m/s. If this wind speed is taken as a 1-min average, then the storm would be a category 1 hurricane. If this 39 m/s wind speed is taken to correspond to a 1-h mean value, then the storm would be rated as a category 2 storm; hence, a range of storm categories is given in Table 6.

If the hurricanes given in Table 6 had been categorized by central pressure instead of the estimated maximum wind speed at the time of landfall, there would be a one-to-one correspondence between the scored category and the actual category. Considering that the hurricane categories assigned to the storms by the National Hurricane Center (NHC) and given in Table 6 are based primarily on upper-level wind speeds measured by numerous aircraft coupled with surface-level wind speeds measured at data buoy and Coastal-Marine Automated Network (C-MAN) stations, it is not unreasonable to assume that the errors in hurricane classification (as defined by the peak wind speed) in earlier years, when the quantity and quality of full-scale data were not as high as today, were even more frequent. In general, it is much simpler to determine the minimum central pressure in a hurricane than it is to reconstruct the wind field, and only over the past 2 decades has a

significant effort gone into poststorm hurricane wind field reconstruction. Errors associated with the measurements of wind speed are much greater than those associated with the measurements of central pressure. Note that the writers do not advocate defining the intensity of a hurricane by the central pressure, but they simply note that the use of the measured central pressure to define a storm category appears to yield more consistent and error-free categorizations.

Based on central pressure, the simulation estimates an average of 1.99 hurricane strikes/year on the U.S. mainland. Based on the sustained wind speed, the simulation yields an average of 1.91 strikes/year. The average annual number of direct hurricane hits given in Hebert et al. (1997) is 1.63, but this value counts a storm that makes landfall twice along the coastline as only one hurricane (e.g., Hurricane Andrew in South Florida and Louisiana, and Hurricane Erin along the Florida Peninsula and subsequently the Florida Pan Handle). As indicated in the HURDAT database, approximately 25% of tropical storms and/or hurricanes that make landfall once along the U.S. coastline make landfall again somewhere else along the coast, indicating the average annual number of strikes is higher than 1.63.

In the case of the category 4 and higher storms, the simulated average annual landfall rate derived from the wind speed is one storm every 7 years, or one storm every 4 years if central pressure is used to define storm category. These values are similar to the NHC estimated landfall rate of about one category 4 or higher storm about every 6 years. The overall agreement between the historical and the simulated occurrence of these relatively infrequent but damaging storms lends further confidence to the simulation model, and this type of regional calibration is not possible with the traditional single-point hurricane simulation techniques used in the past.

## PREDICTED WIND SPEED VERSUS RETURN PERIOD FOR COASTAL AND INLAND STATIONS

Using the storm track simulation methodology described earlier, modeling  $R_{\max}$  and  $B$  using (7) and (16), respectively, combined with the wind field and gust factor models described in Vickery et al. (2000) and Vickery and Skerlj (unpublished manuscript, 2000), 20,000 years of storms were simulated. When a simulated storm is within 250 km of MP, the peak gust wind speeds are recorded at 15-min intervals, with the largest wind speed in each of 16 directions and the largest overall being retained. Upon completion of a 20,000-year simulation, the wind speed data are rank ordered and then used to define the wind speed probability distribution conditional on a storm being within 250 km of the site,  $P(v > V)$ . The probability that the tropical cyclone wind speed (independent of direction) is exceeded during time period  $t$  is

$$P_t(v > V) = 1 - \sum_{x=0}^{\infty} P(v < V|x)p_t(x) \quad (17)$$

where  $P(v < V|x)$  = probability that velocity  $v$  is less than  $V$  given that  $x$  storms occur; and  $p_t(x)$  = probability of  $x$  storms occurring during time period  $t$ . From (17), with  $p_t(x)$  defined as Poisson's and defining  $t$  as 1 year, the annual probability of exceeding a given wind speed is

$$P_a(v > V) = 1 - \exp[-vP(v > V)] \quad (18)$$

where  $v$  represents the average annual number of storms approaching within 250 km of the site (i.e., the annual occurrence rate).

In the directional case, the probability of exceeding a given wind speed during time period  $t$  within the directional sector  $\theta \pm \Delta\theta/2$  is

$$P_\theta(v > V) = 1 - [n(\theta)/N] \sum_{x=0}^{\infty} P_\theta(v < V|x)p_t(x) \quad (19)$$

where  $P_\theta(v < V|x)$  = probability that velocity  $v$  is less than  $V$  given that  $x$  storms occur and produce a wind speed within the directional segment  $\theta \pm \Delta\theta/2$ ;  $n(\theta)$  = number of storms producing a wind speed within the sector; and  $N$  = total number of simulated storms.

## Comparisons to Results of Other Studies

Fig. 10 presents a comparison of the 50- and 100-year return period wind speeds at 61 MPs along the U.S. coastline (see Fig. 2 for MP locations). The extreme wind speeds are obtained using the new simulation methodology coupled with the wind field model described in Vickery and Twisdale (1995a) and using the results of the study described by Vickery and Twisdale (1995b), which uses the same hurricane wind field model but a different simulation approach. The comparisons given in Fig. 10 show the effect of the new simulation methodology, including the new model for  $R_{\max}$ , on the prediction of wind speeds. All wind speeds presented in Fig. 10 are representative of over water values at the coastline. On average, the new simulation technique produces wind speeds that are slightly lower than those given in Vickery and Twisdale (1995b). In no case are the wind speeds obtained using the new approach more than 6% lower than those given in Vickery and Twisdale (1995b). The most significant difference occurs at MP 250, where the new approach yields wind speeds 8–10% higher than those obtained by Vickery and Twisdale (1995b).

Comparisons of the 50- and 100-year return period wind speeds predicted in this study, which uses the new hurricane simulation technique and the wind field and gust factor models described by Vickery et al. (2000) and Vickery and Skerlj (unpublished manuscript, 2000), with those predicted by Vickery and Twisdale (1995b) and Georgiou (1985) are given in Figs. 11 and 12, respectively. Differences between the predictions of wind speed for the various models is a combined effect of the wind field model, filling models,  $R_{\max}$  modeling, site-specific hurricane statistics modeling, and track modeling technique.

The comparisons of the 50- and 100-year return period peak gust wind speeds given in Fig. 11 show relatively little difference (i.e., < 10%) between the new results and the results of Vickery and Twisdale (1995b) for MP 900–2,400. Sensitivity studies performed during the investigation indicate that the lower wind speeds produced by the current model for lo-

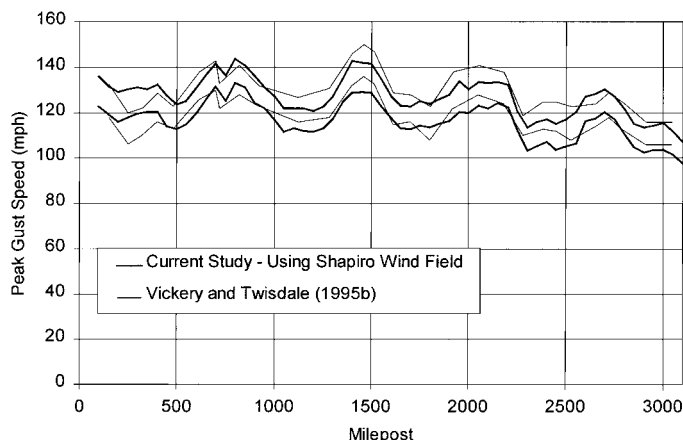
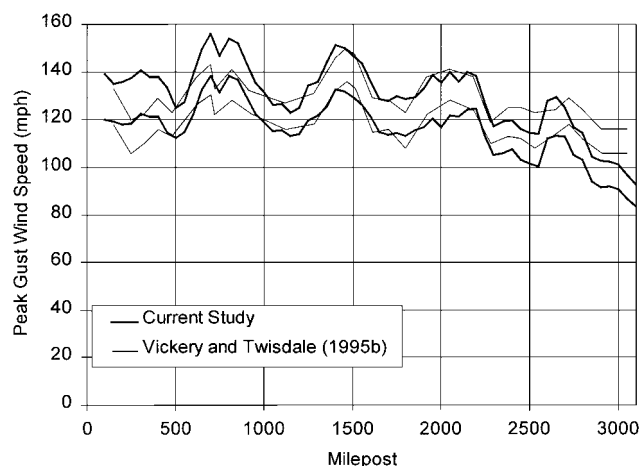
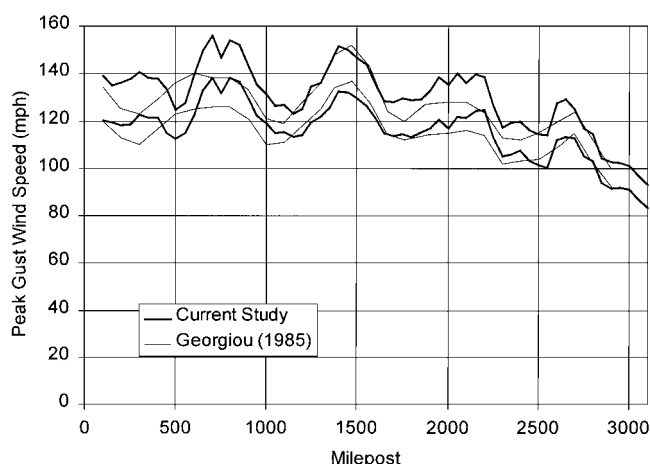


FIG. 10. Comparisons of 50- and 100-Year Return Period Peak Gust Wind Speeds Obtained in Study Using Vickery and Twisdale (1995a) Wind Field Model to Speeds Obtained by Vickery and Twisdale (1995b)



**FIG. 11. Comparisons of 50- and 100-Year Return Period Peak Gust Wind Speeds Obtained in Study to Speeds Obtained by Vickery and Twisdale (1995b)**



**FIG. 12. Comparisons of 50- and 100-Year Return Period Peak Gust Wind Speeds Obtained in Study to Speeds Obtained by Georgiou (1985)**

cations north of MP 2,400 are associated with the decreasing value of the Holland profile parameter in this area. The higher wind speeds resulting from the current model for MP <900 are produced by a combination of the differences in the mean values of the central pressures (Fig. 3) and the differences in the wind field models.

The comparisons of the 50- and 100-year return period peak gust wind speeds obtained in this study to those obtained by Georgiou (1985) are given in Fig. 12. As in the comparison to the Vickery and Twisdale (1995b) results, the largest differences seen here occur for MPs less than about 1,000, where the differences are similar to those evident in Fig. 11. For MPs 1,800–2,400, the results from the current study are greater than the results from Georgiou, and for MPs 2,400 and greater, the results are again similar.

### Predictions of Wind Speeds at Coastal and Inland Locations in the United States

Simulated wind speeds (and hence wind speed probability distributions) were derived at a total of 208 locations in the United States. The stations include the 61 U.S.-based coastal MPs defined earlier and 147 other stations nominally located at 50, 100, and 200 km from the coast. Some additional coastal locations are added along the mid-Atlantic coastline. Results are presented for return periods of 50, 100, and 500 years in Fig. 13. The wind speed contours are representative of wind

speeds at 10 m above ground in open terrain. Therefore, the wind speed contours shown at the coast are lower values than those given in Figs. 11 and 12, which are over water values.

The regions experiencing the highest 50-, 100-, and 500-year return period wind speeds are centered near the Mississippi Delta and the South Florida region. For return periods of 50 and 100 years, the peak predicted wind speeds in the South Florida area are less than those near the Mississippi Delta region. These lower wind speeds around South Florida are consistent with the lower values of the mean central pressure difference near South Florida as compared to the Mississippi Delta area (Fig. 3). For longer return periods, the predicted wind speeds in the South Florida region become higher than those in the Mississippi Delta region. This more rapid increase in wind speed with return period is associated with the higher RMS central pressure differences (hence longer tails in the statistical distributions) seen in the South Florida region as compared to the Mississippi Delta region (Fig. 3). The larger central pressure difference effect is amplified by the fact that these more intense storms are likely to be associated with larger  $B$  values.

### Areawide Simulations for South Florida

Using the hurricane simulation model, combined with a grid size of  $0.05^\circ \times 0.05^\circ$  covering the populated areas of Dade and Broward counties, a 20,000-year simulation was performed. Using this simulation one retains the maximum simulated wind speed recorded at each grid point located within a populated region of the county. Using this wind speed data, plots of wind speed versus return period are generated comparing the single-point wind speed exceedance probability for a typical point in the region to the exceedance probabilities for points anywhere in Dade County, anywhere in Broward County, and anywhere in either county. Results are given in Fig. 14. Note that the storm categories given in Fig. 14 are defined by the peak gust wind speeds on land as given in Table 5. For example, the 191-mph peak gust wind speed over land corresponding to the lower threshold of the category 5 storm results from a 1-min mean wind speed of 155 mph over water. As indicated in Fig. 14, category 4 hurricane wind speeds can be expected to be exceeded on average about once every 70 years somewhere within the region encompassing Dade and Broward counties. Category 5 wind speeds are expected to be exceeded on average about once every 300 years. Hurricane Andrew, with peak gust wind speeds (on land, open terrain) of 165–170 mph is estimated to have a return period of about 120 years for the region encompassing both Dade and Broward counties.

Predicted 50-, 100-, and 500-year return period single-point peak gust wind speeds also are given in Fig. 14 for the results given by Batts et al. (1980), Georgiou (1985), and Vickery and Twisdale (1995b).

### SUMMARY

A new simulation model has been developed that models the entire track of a tropical storm in the Atlantic Basin. The model is validated through comparisons to historical data showing its validity along the U.S. and Mexican coastline. The new modeling approach allows the storms to curve and change speed and intensity as they move and is able to reproduce the continuously varying statistics associated with central pressure, heading, etc., along the U.S. coastline. The model is an improvement over earlier hurricane simulation techniques because it eliminates the problems associated with the selection of a subregion from which to derive the statistical distributions needed in traditional simulation models. In traditional models, the use of large areas to derive the hurricane statistics will

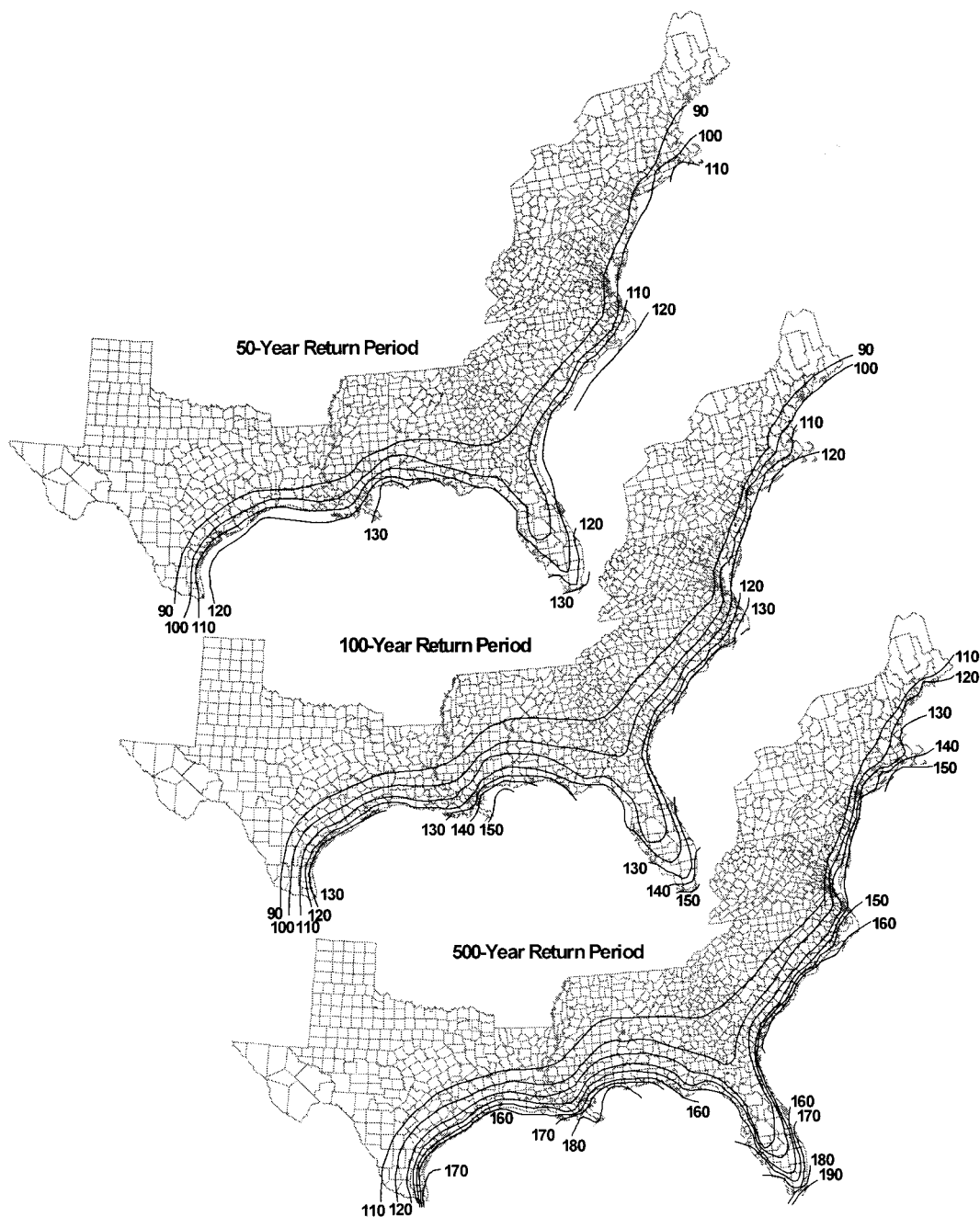


FIG. 13. 50-, 100-, and 500-Year Return Period Peak Gust Wind Speeds in Open Terrain

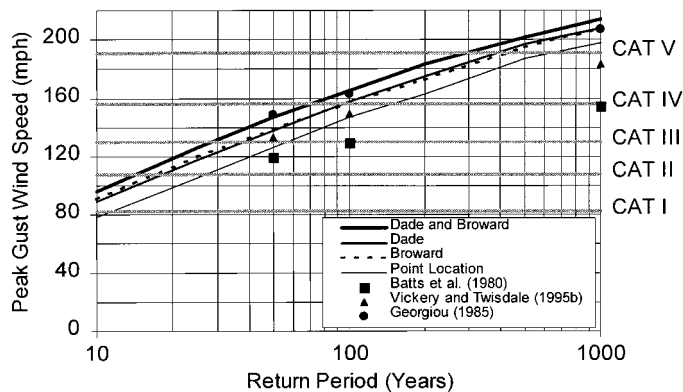


FIG. 14. Comparison of Predicted Wind Speed for Point Location in Dade County and for Regions Encompassed by Dade and Broward Counties (CAT = Category)

smear any local climatological features that are inherently reproduced in the new simulation method.

The prime advantage of this new modeling approach compared to the traditional approaches is the ability to properly model hurricane wind risk over large regions, within which the hurricane climatology can vary significantly. This is useful for assessing the risk of large-scale systems, such as transmission line systems, for examining the risk to facilities that may be located in multiple states, or for addressing insurance issues, where policies may be distributed along the entire coastline.

#### ACKNOWLEDGMENTS

The research described in this paper was partly supported by the National Science Foundation, Washington, D.C., under a Phase II Small Business Innovation Research Grant, ISI 9304222, and by the National Association of Home Builders, Washington, D.C.

The results, findings, and conclusions of this study are those of the writers and do not represent those of the sponsors.

## APPENDIX. REFERENCES

- American National Standards Institute (ANSI). (1982). "Minimum design loads for buildings and other structures." *ANSI A58.1*, New York.
- ASCE. (1990). "Minimum design loads for buildings and other structures." *ASCE 7-88*, New York.
- ASCE. (1996). "Minimum design loads for buildings and other structures." *ASCE 7-95*, New York.
- Batts, M. E., Cordes, M. R., Russell, L. R., Shaver, J. R., and Simiu, E. (1980). "Hurricane wind speeds in the United States." *Rep. No. BSS-124*, Nat. Bureau of Standards, U.S. Department of Commerce, Washington, D.C.
- Caribbean Community Secretariat (CCS). (1985). "Structural design requirements: Wind load." *Caribbean uniform building code*, Part 2, Sect. 2, Georgetown, Guyana.
- Chouinard, L. E., Liu, C., and Cooper, C. K. (1997). "Model for severity of hurricanes in Gulf of Mexico." *J. Wtrwy., Port, Coast., and Oc. Engrg.*, ASCE, 123(3), 120–129.
- Darling, R. W. R. (1991). "Estimating probabilities of hurricane wind speeds using a large-scale empirical model." *J. Climate*, 4(10), 1035–1046.
- Emmanuel, K. A. (1988). "The maximum intensity of hurricanes." *J. Atmospheric Sci.*, 45, 1143–1155.
- Georgiou, P. N. (1985). "Design windspeeds in tropical cyclone-prone regions." PhD thesis, Fac. of Engrg. Sci., University of Western Ontario, London, Ont., Canada.
- Georgiou, P. N., Davenport, A. G., and Vickery, B. J. (1983). "Design wind speeds in regions dominated by tropical cyclones." *J. Wind Engrg. and Industrial Aerodynamics*, Amsterdam, The Netherlands, 13(1), 139–152.
- Hebert, P. J., Jarrell, J. D., and Mayfield, B. M. (1997). "The deadliest, costliest, and most intense United States hurricanes of this century (and other frequently requested hurricane facts)." *NOAA Tech. Memo. NWS-TPC-1*, U.S. Department of Commerce, Washington, D.C.
- Ho, F. P., Su, J. C., Hanevich, K. L., Smith, R. J., and Richards, F. P. (1987). "Hurricane climatology for the Atlantic and Gulf coasts of the United States." *NOAA Tech. Rep. NWS38*, Federal Emergency Management Agency, Washington, D.C.
- Holland, G. J. (1980). "An analytic model of the wind and pressure profiles in hurricanes." *Monthly Weather Rev.*, 108(8), 1212–1218.
- Houston, S. H., Powell, M. D., and Dodge, P. P. (1997). "Surface wind fields in 1996 Hurricanes Bertha and Fran at landfall." *Proc., 22nd Conf. on Hurricanes and Tropical Meteorology*, American Meteorological Society, Boston, 92–93.
- Jarvinen, B. R., Neumann, C. J., and Davis, M. A. S. (1984). "A tropical cyclone data tape for the North Atlantic Basin 1886–1983: Contents, limitations and uses." *NOAA Tech. Memo. NWS-NHC-22*, U.S. Department of Commerce, Washington, D.C.
- Neumann, C. J. (1991). "The National Hurricane Center Risk Analysis Program (HURISK)." *NOAA Tech. Memo. NWS-NHC-38*, U.S. Department of Commerce, Washington, D.C.
- Powell, M. D. (1987). "Changes in the low-level kinematic and thermodynamic structure of Hurricane Alicia (1983) of landfall." *Monthly Weather Rev.*, 115, 75–99.
- Powell, M. D., Dodge, P. P., and Black, L. B. (1991). "The landfall of Hurricane Hugo in the Carolinas: Surface wind distribution." *Weather and Forecasting*, 6, 379–399.
- Powell, M. D., and Houston, S. H. (1996). "Hurricane Andrew's landfall in South Florida—Part II: Surface wind fields and potential real-time applications." *Weather and Forecasting*, 11(3), 329–349.
- Powell, M. D., and Houston, S. H. (1998). "Surface wind fields of 1995 Hurricanes Erin, Opal, Luis, Marilyn, and Roxanne at landfall." *Monthly Weather Rev.*, 126, 1259–1273.
- Russell, L. R. (1968). "Probability distribution for Texas Gulf Coast hurricane effects of engineering interest." PhD thesis, Stanford University, Stanford, Calif.
- Russell, L. R. (1971). "Probability distributions for hurricane effects." *J. Wtrwy., Harb. and Coast. Engrg. Div.*, ASCE, 97(1), 139–154.
- Standards Association of Australia (SAA). (1989). "Loading code, Part 2—Wind forces." *AS1170 Part 2*, Sydney, Australia.
- Thompson, E. F., and Cardone, V. J. (1996). "Practical modeling of hurricane surface wind fields." *J. Wtrwy., Port, Coast., and Oc. Engrg.*, ASCE, 122(4), 195–205.
- Vickery, P. J., Skerlj, P. F., Steckley, A. C., and Twisdale, L. A. (2000). "Hurricane wind field model for use in hurricane simulations." *J. Struct. Engrg.*, ASCE, 126(10), 1203–1222.
- Vickery, P. J., and Twisdale, L. A. (1995a). "Wind-field and filling models for hurricane wind-speed predictions." *J. Struct. Engrg.*, ASCE, 121(11), 1700–1709.
- Vickery, P. J., and Twisdale, L. A. (1995b). "Prediction of hurricane wind speeds in the United States." *J. Struct. Engrg.*, ASCE, 121(11), 1691–1699.